EUROPEAN ORGANIZATION FOR NUCLEAR RESEARCH

Proposal to the ISOLDE and Neutron Time-of-Flight Committee

Single-particle behaviour towards doubly-magic ^{24}O - ^{27}Na(d,p)^{28}Na in inverse kinematics

January 5, 2022

D. K. Sharp[1], S. J. Freeman[1], S. A. Bennett[1], F. Browne[2], P. A. Butler[3],
W. N. Catford[4], J. Chen[5], D. Clarke[1], L. P. Gaffney[3], K. Garrett[1], C. R. Hoffman[5],
B. P. Kay[5], Th. Kröll[6], M. Labiche[7], R. S. Lubna[8], P. T. MacGregor[1], B. Olaizola[2],
R. D. Page[2], R. Raabe[9], S. Reeve[1] , T. L. Tang[10], and K. Wimmer[11]

[1]*School of Physics and Astronomy, The University of Manchester, Manchester, M13 9PL, UK*
[2]*ISOLDE, CERN, CH-1211 Geneva 23, Switzerland*
[3]*Oliver Lodge Laboratory, University of Liverpool, Liverpool, L69 7ZE, UK*
[4]*Department of Physics, University of Surrey, Guildford, GU2 5XH, UK*
[5]*Physics Division, Argonne National Laboratory, Argonne, Illinois 60439, USA*
[6]*Institut für Kernphysik, Technische Universität Darmstadt, 64289 Darmstadt, Germany*
[7]*STFC Daresbury Laboratory, Daresbury, Warrington, WA4 4AD, UK*
[8]*FRIB, East Lansing, MI 48824, USA*
[9]*KU Leuven, Instituut voor Kern- en Stralinsfysica, 3001 Leuven, Belgium*
[10]*Department of Physics, Florida State University, Tallahassee, FL 32306 USA*
[11]*GSI Helmholtzzentrum für Schwerionenforschung GmbH, Plankstrasse 1, 64291 Darmstadt, Germany*

Spokesperson: D. K. Sharp (david.sharp@manchester.ac.uk)
Co-spokesperson: S. J. Freeman (sean.freeman@manchester.ac.uk).
ISOLDE contact: Bruno Olaizola (bruno.olaizola@cern.ch)

Abstract: We propose a measurement of the ^{27}Na(d,p)^{28}Na reactions in inverse kinematics using the ISOLDE Solenoidal Spectrometer. The aim of the measurement is to characterise the neutron single-particle trends outside the $N = 16$ isotones towards doubly-magic ^{24}O. The neutron-adding reaction will provide spectroscopic overlaps for the $0d_{3/2}$, $0f_{7/2}$, $1p_{3/2}$ and $1p_{1/2}$ orbitals. The energy differences between the $0d_{3/2}$ and $0f_{7/2}$ orbitals define the $N = 20$ shell closure. These data will provide information regarding the evolution of the $N = 16$ and $N = 20$ shell closures and the relative strengths of the important monopole interactions, for comparison with modern shell-model predictions. We request 15 shifts of beam time for this measurement.

1   Physics case

Single-particle characteristics underlie many aspects of nuclear structure. The study of single-particle structure in light neutron-rich systems has led to discoveries of dramatic changes, leading to the weakening and appearance of shell closures. These include the disappearance of the $N = 20$ shell-closure and emergence of one at $N = 16$ [1, 2] and the emergence of $N = 32, 34$ sub-shell closures in calcium isotopes [3, 4, 5]. As Z decreases along the $N = 16$ isotones, there is evidence that $N = 20$ becomes quenched, with a new $N = 16$ shell closure emerging in ^{24}O making this a doubly magic nucleus [1, 2]. This can be qualitatively explained in terms of the effect of the different proton-neutron monopole interactions. As protons fill the $\pi d_{5/2}$ orbital from oxygen to silicon the $\nu d_{3/2}$ experiences a larger attractive force as the $0d_{5/2} - 0d_{3/2}$ interaction is larger than the $0d_{5/2} - 0f_{7/2}$ and $0d_{5/2} - 1p_{3/2}$ interactions, reducing its energy, and forming the $N = 20$ shell gap to the pf shell [6].

The weakening of the $N = 20$ shell closure also has consequences for the region of nuclei around ^{32}Mg ($Z \sim 12$, $N \sim 20$), known as the "island of inversion" (IOI). This is so-called because ground states and low-lying excitations originating from intruder configurations have been observed in these nuclei. Intruder configurations are those resulting from the promotion of one or more neutrons across a shell closure, in this case $N = 20$, generating neutron holes in the orbits below the closed shell. This phenomenon was first identified through anomalous ground-state binding energies of Mg, Na and Ne isotopes [7, 8]. These intruder configurations, and the onset of deformation that accompanies them, are a result of a weakening shell closure.

The difference between the $0d_{3/2}$ and the $0f_{7/2}$ (or $1p_{3/2}$) single-particle energies is indicative of the $N = 20$ shell closure. The difference that emerges in the $1s_{1/2}$ and $0d_{3/2}$ orbitals signifies the emergence of $N = 16$ as a shell gap. The size of these gaps, and how they change, characterises this unique region of the nuclear chart. Along the $N = 17$ isotonic chain transfer data exist for ^{33}S (e.g. [9, 10]), ^{31}Si (e.g. [11]), ^{29}Mg (e.g. [12]) and ^{27}Ne (e.g. [13]), with the most recent data on ^{29}Mg taken by this collaboration. We have additionally made a recent measurement of the ^{29}Al$(d,p)^{30}$Al reaction in inverse kinematics using HELIOS at Argonne National Laboratory, where the data are currently under analysis. A reduction in the $N = 20$ shell gap has been observed between ^{31}Si and ^{29}Mg, which appears well reproduced by shell-model calculations as shown in Figure 1. The shell-model calculations used in Ref. [12] show that ^{29}Mg lies at a transitional point in terms of the behaviour of neutrons, where in lighter $N = 16$ nuclei there is a change in the occupancy of the $d_{3/2}$ and $s_{1/2}$ neutron orbitals - potentially arising due to the emergence of the $N = 16$ shell closure. Studying the occupancies and single-particle centroids of these nuclei would be informative in confirming this behaviour. The relative changes in both the observed summed single-particle strength and centroids of these orbitals in ^{27}Na, compared to heavier isotones, would provide details on the relative strengths of the
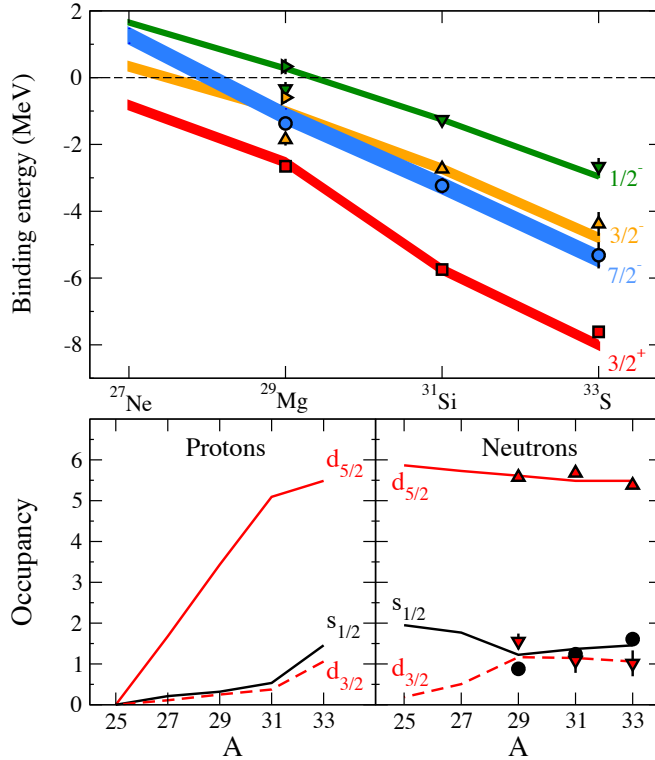
Figure 1: Figure taken from Ref. [12]. (Top) Binding energy of single-particle centroids for $J^\pi = 3/2^+$ ($\square$), $7/2^-$ ($\bigcirc$), $3/2^-$ ($\triangle$) and $1/2^-$ ($\triangledown$) in $N = 17$ isotones. Centroids for $J^\pi = 1/2^-, 3/2^-$ including states above 5.5 MeV are denoted by $\triangleright$. Bands represent calculations using the FSU interaction [15, 16], with widths representing experimental uncertainties in ^{31}Si, onto which they are shifted. (Bottom) Calculated nucleon occupancies for $N = 17$ isotones from the FSU interaction (lines). Symbols represent neutron occupancies extracted from the data.

monopole interactions between the different neutron orbitals and the $d_{5/2}$ protons. This information is lacking still in efforts to well describe this changing region of the nuclear chart.

The beam intensities at HIE-ISOLDE are sufficient to probe states in ^{28}Na, via the ^{27}Na(d,p) reaction in inverse kinematics, allowing us to track these single-neutron excitations along $N = 17$. The ^{27}Na$(d,p)^{28}$Na reaction has never been measured previously, with only limited spin assignments on tentative states from comparisons of β-decay and β-delayed spectroscopy measurements to shell-model calculations (e.g. [17]), and the first 2^+ has been populated in Coulomb excitation [18]. More recently the spectroscopy of ^{28}Na was investigated by means of β decay of ^{28}Ne and in-beam γ-ray spectroscopy [19]. Tentative assignments of a negative-parity $J^\pi = 2^- - 4^-$ multiplet around 1.5 MeV were proposed, arising from the $\pi d_{5/2} - \nu p_{3/2}$ coupling, and a 5^- state around 2.5 MeV, likely arising from the $\pi d_{5/2} - \nu f_{7/2}$ coupling. This suggests that the $\nu p_{3/2}$ is now lower in energy than the $\nu f_{7/2}$, when compared to nearer stability. The aim of the proposed measurement would be to confirm the negative-parity nature of these states and assess the relative

3

single-particle strength distributions of the $d_{3/2}$, $f_{7/2}$ and $p_{3/2}$ orbitals.

The ISOLDE Solenoidal Spectrometer allows states up to and beyond the neutron separation threshold to be observed, since γ-rays are not required to extract the proton yields. This will allow us to probe the distribution of single-particle strength up to and beyond the neutron separation energy, which lies at 3542 keV. The confirmation of the negative-parity states should be an achievable goal of this measurement - as well as probing any potential strength lying at higher excitation in order to identify strength corresponding to $\pi d_{5/2} - \nu p_{1/2}$ coupling. These data, when combined with our data on ^{30}Al and ^{29}Mg, will provide a systematic picture on the neutron single-particle behaviour along these isotones - towards ^{24}O, investigating the weakening of the $N = 20$ shell closure and benchmarking shell-model interactions in describing these changes.
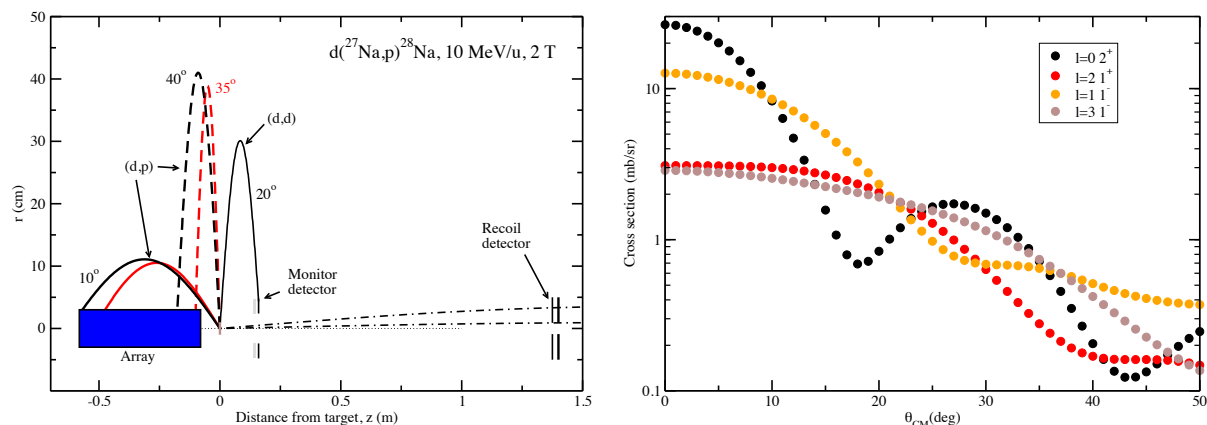
2   Experimental details

Figure 2: (Left) Proposed experimental set-up within the solenoidal spectrometer. Distances are relative to the target position. For the (d,p) reaction, the black lines represents protons from population of the ground state whilst the red lines are protons from population of a theoretical state at the neutron separation energy of ^{27}Na. The dash-dot lines represent the path of the residual beam-like nuclei. All angles are given in centre-of-mass. See text for detailed description. (Right) Angular distributions calculated using the DWBA for $\ell=0\text{-}3$ transfer.

Transfer reactions are the ideal tool for studying single-particle properties of nuclei. Under the right experimental conditions, they provide selective access to single-particle states. The occupancies and vacancies of the active single-particle orbitals, as well as their effective single-particle energies, can be deduced from transfer data. These are key ingredients for explaining the roles of different components of the nucleon-nucleon interaction in the evolution of single-particle structure.

Reaction and beam energy—We propose to measure single-neutron transfer in inverse kinematics to probe the single-particle structure in neutron-rich ^{28}Na at an incident beam energy of 10 MeV/u. At these energies, the angular distributions for

4

transfer to final states of differing ℓ allow distinct assignments of the transferred angular momentum to be made, see Fig. 2. For this system, there are multiple allowed ℓ transfers to the same final state. Low-spin positive-parity states can be populated by $\ell = 0$ or 2 transfer, with $\ell = 1$ or 3 transfer populating the negative-parity states. The beam-time request accounts for the need to fit combinations of multiple angular distributions to the data. Figure 3 shows combinations of angular distributions for a range of different spectroscopic factors, where the ratio given is that of the spectroscopic factors for the two different ℓ contributing to the distribution. The range of these values covers those expected in the proposed measurement. These have been normalized for comparison and separately pure $\ell = 2$ and 3 distributions are plotted, as some states will be populated via a single ℓ transfer. It can be seen that the identification of positive- and negative-parity states is possible, with differing shapes for different ratios of ℓ contribution over the angular range probed, at this beam energy. A statistical uncertainty of better than 10% is required in the worse case, within the goals of the beam time request that is set out below. States of combined ℓ are also distinguishable from those populated via a single ℓ transfer, within the statistical uncertainties of the measurement. Though cross sections for the population of some states is higher at lower beam energies, the resulting angular coverage of the array and recoil detectors is more limited at forward angles, impacting on the ability to make good ℓ assignments for the states of interest. The chosen beam energy is a good compromise between angular coverage and yield.
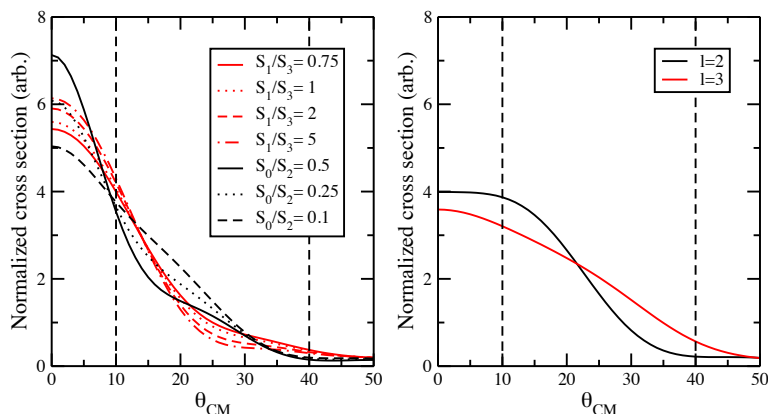

Figure 3: (Left) Normalized angular distributions for combinations of ℓ transfer to final states. Distributions for transfer to positive-parity states are given in black with those to negative parity in red. Distributions for a range of expected ratios of spectroscopic factors are given. (Right) Normalized distributions for $\ell=2$ and 3 transfers for comparison. The dashed vertical lines indicates the average angular coverage of the ISS array.

ISOLDE Solenoidal Spectrometer—In inverse kinematics a heavy beam is incident on a light target, in this case deuterated polyethylene (CD_2). The protons from the (d,p) reaction at the forward centre-of-mass angles of interest are emitted at backwards laboratory angles, relative to the incident beam direction. We intend to use the ISOLDE Solenoidal Spectrometer (ISS) in order to momentum analyse the outgoing protons, measuring energies, and yields of protons populating final states in the residual nuclei

of interest. The expected level density, using the states identified in Ref. [19] and a comparison to the shell-model calculations for states populated via one-neutron transfer, are shown in Figure 4. The expected energy resolution of 100 keV FWHM would be sufficient to resolve the majority of the states of interest, with the exception of two known doublets, though not resolving these will not negatively impact the physics goals.
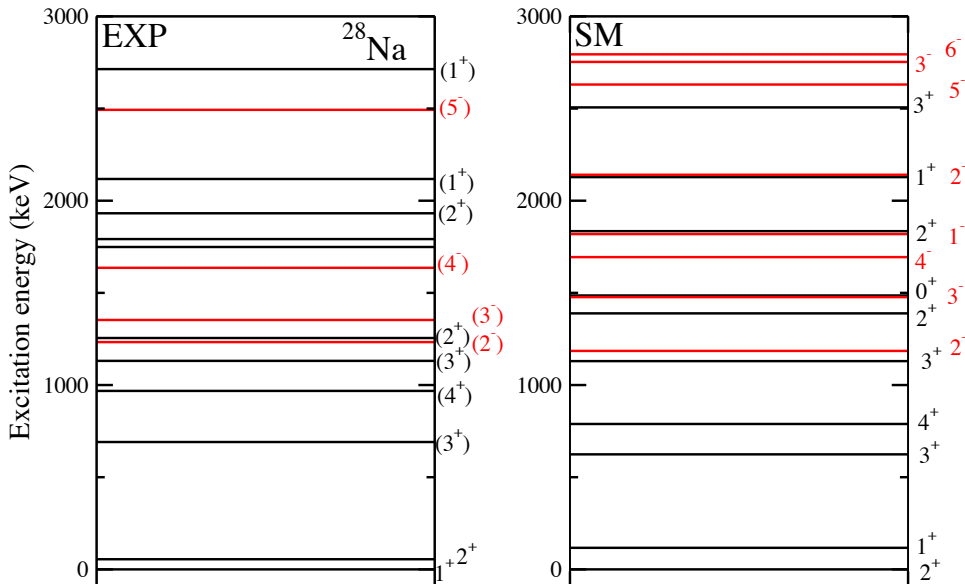

Figure 4: (Left) Levels identified in ^{28}Na by β-decay and in-beam γ-ray spectroscopy [19] along with tentative assignments from that work. Positive-parity states are given in black with negative-parity in red. (Right) Levels in ^{28}Na calculated using the FSU interaction [15].

Experimental set-up—The setup for the ^{27}Na(d,p) measurement is shown in Figure 2. The silicon array will be positioned -8 cm from the target as measured to the nearest detector edge, covering a range in z from the target of -8 to -58 cm. The solenoid field will be set at 2 T. With these settings, protons emitted at $10° < \theta_{cm} < 35°$ will be incident on the array for all states up to the neutron-separation energy. This range of angles covers the first maxima of the angular distributions for $\ell = 1 - 3$. Spectroscopic factors are best extracted from the first peak, or as near as possible, of the angular distributions where the assumptions implicit in DWBA are most valid. Elastically-scattered deuterons will be detected in an annular silicon detector positioned at $z = +18$ cm to enable an absolute normalisation. At a position $z = +140$ cm from the target, an annular ΔE-E telescope will be located. This will detect the recoiling beam-like particles in order to clean the spectra of reactions on beam contaminants and from fusion-evaporation reactions on the carbon in the target. It will also provide a timing reference for the identification of protons in the array, using their cyclotron period as a means of particle identification. This detector has previously been used with beams in this mass region at intensities of $\sim 10^6$ pps without any observation of pile-up or other rate limiting effects.

Beam time request—A beam intensity of 3×10^5 pps of ^{27}Na has been assumed based on the yield database and an assumption of a proton current of 1 μA and 4% transmission through HIE-ISOLDE. Contamination of stable ^{27}Al is expected up to the 50% level. This can be separated in the recoil detectors of ISS to identify the reaction of interest. The array has an efficiency of 70% in the azimuthal angle and 95% in the theta angle. Protons in the angular range $10° < \theta_{cm} < 35°$ will be incident on the array. The CD$_2$ targets will be $\sim$100 μg/cm^2 thick. Cross sections were estimated using the finite-range DWBA code Ptolemy and optical-model parameters of An and Cai [21] and Koning and Delaroche [22] for the deuteron and proton, respectively. Under these assumptions we estimate that a minimum of $\sim$115 counts per day for transfer to the negative-parity states of interest will be observed in the whole array, using spectroscopic factors from the FSU calculations [15]. The predicted spectroscopic factors for the $\ell = 1$ and 3 components of the $J^\pi = 1^- - 4^-$ multiplet are in the range $S = 0.05 - 0.4$. A maximum of an 8% statistical uncertainty in an angular bin is required in order to identify the different ℓ contributions to a negative-parity state at the level of $S = 0.1$, where the total counts are divided between ten angular bins. This level of statistics is achieveable for all but the lowest spin ($J^\pi = 1^-$) within 15 shifts and as such we request **15 shifts** of beam on target. This also includes time for optimising the delivery of beam onto the target position. A lower number of angular bins can be used to obtain this level of statistics for the low spin states. This level of statistics is also sufficient to robustly identify the parity of the populated states.

Summary of requested protons: 15 shifts of protons are requested for this measurement.

References

[1] A. Ozawa, *et al.,* Phys. Rev. Lett. **84**, 5493 (2000).
[2] C. R. Hoffman, *et al.,* Phys. Lett. B **672**, 17 (2009).
[3] D. Steppenbeck, *et al.,* Nature **502**, 207 (2013).
[4] S. Michimasa, *et al.,* Phys. Rev. Lett **121**, 022506 (2018).
[5] S. Chen, *et al.,* Phys. Rev. Lett **123**, 142501 (2019).
[6] T. Otsuka, *et al.,* Phys. Rev. Lett. **95**, 232502 (2005).
[7] C. Thibault, *et al.,* Phys. Rev. C **12**, 644 (1975).
[8] E. K. Warburton, J. A. Becker, and B. A. Brown Phys. Rev. C **41**, 1147 (1990).
[9] M. C. Mermaz,*et al.,* Phys. Rev. C **4**, 1778 (1971).
[10] R. Liljestrand, *et al.,* Phys. Rev. C **11**, 1570 (1975).
[11] Š. Piskoř, *et al.,* Nucl. Phys. A **662**, 112 (2000).
[12] P. T. MacGregor *et al.,* Phys. Rev. C **104**, L051301 (2021).
[13] S. M. Brown, *et al.,* Phys. Rev. C **85**, 011302 (2012).
[14] G. Burgunder, *et al.,* Phys. Rev. Lett. **759**, 042502 (2014).
[15] R. S. Lubna (Priv. Comm).
[16] R. S. Lubna, *et al.,* Phys. Rev. C. **100** 034308 (2019).

[17] V. Tripathi, *et al.,* Phys. Rev. C. **73** 054303 (2006).

[18] B. V. Pritychenko, *et al.,* Phys. Rev. C. **66** 024325 (2002).

[19] A. Pepailleur, *et al.,* Phys. Rev. C. **92** 054309 (2015).

[20] M. H. Macfarlane and S. C. Pieper, ANL-76-11 Rev. 1, ANL Report (1978).

[21] H. An and C. Cai Phys. Rev. C **73**, 054605 (2006).

[22] A. J. Koning and J. P. Delaroche Nuc. Phys. A. **713**, 231 (2003).

Appendix

DESCRIPTION OF THE PROPOSED EXPERIMENT

The experimental setup comprises: (The ISOLDE Solenoidal Spectrometer)

Part of the	Availability	Design and manufacturing
ISOLDE Solenoidal Spectrometer	☒ Existing	☒ To be used without any modification
		☐ To be modified
	☐ New	☐ Standard equipment supplied by a manufacturer
		☐ CERN/collaboration responsible for the design and/or manufacturing

HAZARDS GENERATED BY THE EXPERIMENT (if using fixed installation:) Hazards named in the document relevant for the fixed ISS installation.

Additional hazards:

Hazards			
Thermodynamic and fluidic			
Pressure			
Vacuum			
Temperature			
Heat transfer			
Thermal properties of materials			
Cryogenic fluid			
Electrical and electromagnetic			
Electricity			
Static electricity			
Magnetic field	2 T		
Batteries			
Capacitors			
Ionizing radiation			
Target material	Deuterated polyethylene (50-400 μg/cm^2)		
Beam particle type	^{27}Na		
Beam intensity	3×10^5		
Beam energy	10 MeV/u		
Cooling liquids			
Gases			
Calibration sources:	☒		
• Open source	☒ (α calibrations source 4236RP)		
• Sealed source			

• Isotope	^{148}Gd, ^{239}Pu, ^{241}Am, ^{244}Cm		
• Activity	1 kBq, 1 kBq, 1 kBq, 1 kBq = 4 kBq		
Use of activated material:			
• Description			
• Dose rate on contact and in 10 cm distance			
• Isotope			
• Activity			
Non-ionizing radiation			
Laser			
UV light			
Microwaves (300MHz-30 GHz)			
Radiofrequency (1-300 MHz)			
Chemical			
Toxic			
Harmful			
CMR (carcinogens, mutagens and substances toxic to reproduction)			
Corrosive			
Irritant			
Flammable			
Oxidizing			
Explosiveness			
Asphyxiant			
Dangerous for the environment			
Mechanical			
Physical impact or mechanical energy (moving parts)			
Mechanical properties (Sharp, rough, slippery)			
Vibration			
Vehicles and Means of Transport			
Noise			
Frequency			
Intensity			

Physical			
Confined spaces			
High workplaces			
Access to high workplaces			
Obstructions in passageways			
Manual handling			
Poor ergonomics			

Hazard identification:

Average electrical power requirements (excluding fixed ISOLDE-installation mentioned above): N/A